HEDL-SA-1917 FP

CONF-791051--7

BUFFALO LIGHT WATER REACTOR CALCULATIONS

P. A. Ombrellaro, R. A. Bennett, W. N. McElroy

February 1979

Third ASTM Euratom Symposium on Reactor Dosimetry

October 1-5, 1979, Ispra, Italy

HANFORD ENGINEERING DEVELOPMENT LABORATORY
Operated by Westinghouse Hanford Company, a subsidiary of Westinghouse Electric Corporation, under the Department of Energy Contract No. EY-76-C-14-2170

DISCLAIMER

BUFFALO LIGHT WATER REACTOR CALCULATIONS

P.A. Ombrellaro, R.A. Bennett, E.P. Lippincott, C.L. Long

Westinghouse Hanford Company

P.O. Box 1970, Richland, Washington 99352 USA*

INTRODUCTION

An important objective of the light water reactor pressure vessel (LWRPV) surveillance dosimetry program is to validate and calibrate dosimetry and damage analysis techniques as well as to guide required neutron field calculations that are used to correlate changes in material properties with characteristics of the neutron irradiation field. As part of this activity, the Hanford Engineering Development Laboratory (HEDL) performed neutron flux calculations in a model of the light water test reactor of the Nuclear Science and Technology Facility of the State University of New York at Buffalo. The purpose of these calculations was to provide a consistent analysis base for projecting radiation damage produced by one reactor facility to that which would be incurred in another reactor facility.

Space-energy neutron flux distributions in a two-dimensional model of the reactor were calculated using 28-group cross sections in the diffusion theory code, 2DBS [1]. In these calculations the scattering integral of hydrogen was appropriately modified to provide a correct treatment of the slowing down of neutrons by water. The cross sections, mainly derived from Set 300 [2], were spatially self-shielded to account for the heterogeneity effects of pins in the fuel subassembly when treating the fuel subassemblies as homogenized fuel zones in the diffusion theory calculations. The

---

* This work was funded by both Naval Research Laboratory, Thermal Structural Materials Branch, and Reactor Research and Technology Branch, Department of Energy.

spatially self-shielded cross sections were obtained from transport calculations, using the DTF-IV code [3], performed on a unit cell model of the fuel subassembly.

Neutron flux spectra were calculated at various irradiation test positions in two core regions representing irradiation test facilities containing about 8 kg of steel. These were used to calculate integrated fluxes, spectrum-averaged cross sections for the $^{54}Fe(n,p)^{54}Mn$ and $^{58}Ni(n,p)^{58}Co$ reactions and the iron and stainless steel displacement cross sections in the energy range values E>0 MeV, E>0.1 MeV, E>0.5 MeV, and E>1.0 MeV.

CALCULATIONAL MODEL

Reactor Model

A description of the Buffalo LWR was provided by M. Haas, Associate Director of the test facility. The test reactor consists of 36 modules in a light water lattice. Twenty-nine modules of the 36-module array are fuel subassemblies, and each subassembly consists of 25 fuel pins contained in a Zircaloy-2 box. The reactor is controlled by six cadmium, indium and silver control rod blades. At steady-state operation, during which the reactor normally operates at 2 MW, one blade is fully withdrawn and the other five blades are 85 percent withdrawn. The core contains two irradiation facilities, NRL-1 and NRL-2, each consisting of 8 kg of steel.

This information was used to construct a two-dimensional model in which each fuel zone contains one of six fuel compositions characterized by burnups ranging from 436 to 10,474 MWd/T. The atom densities for each fuel composition were obtained from burnup calculations performed with the LASER program [4] on a unit cell model consisting of a fuel pin surrounded by water.

The reactor model used in calculating the flux spectra at the irradiation test positions is the X-Y configuration shown in Figure 1. Each fuel subassembly (containing 25 discrete fuel pins) is treated as a homogeneous region in this model. In this representation, the fine-structured flux that accounts for the spatial heterogeneity effect of the pins when they are treated discretely was neglected to reduce the complexity of the calculation. However, the heterogeneity effects were still accounted for in the flux calculations by using a set of spatially self-shielded, multigroup, effective cross sections. These cross sections were developed to provide the same reaction rates of materials in the homogeneous subassembly as would be obtained for the same materials in the heterogeneous subassembly.

Different fuel zones identified by amount of fuel burnup;

Composition 1 = 10,474 MWd/T Burnup Composition 4 = 3,199 MWd/T Burnup

Composition 2 = 9,046 MWd/T Burnup Composition 5 = 1,266 MWd/T Burnup

Composition 3 = 6,311 MWd/T Burnup Composition 6 = 436 MWd/T Burnup

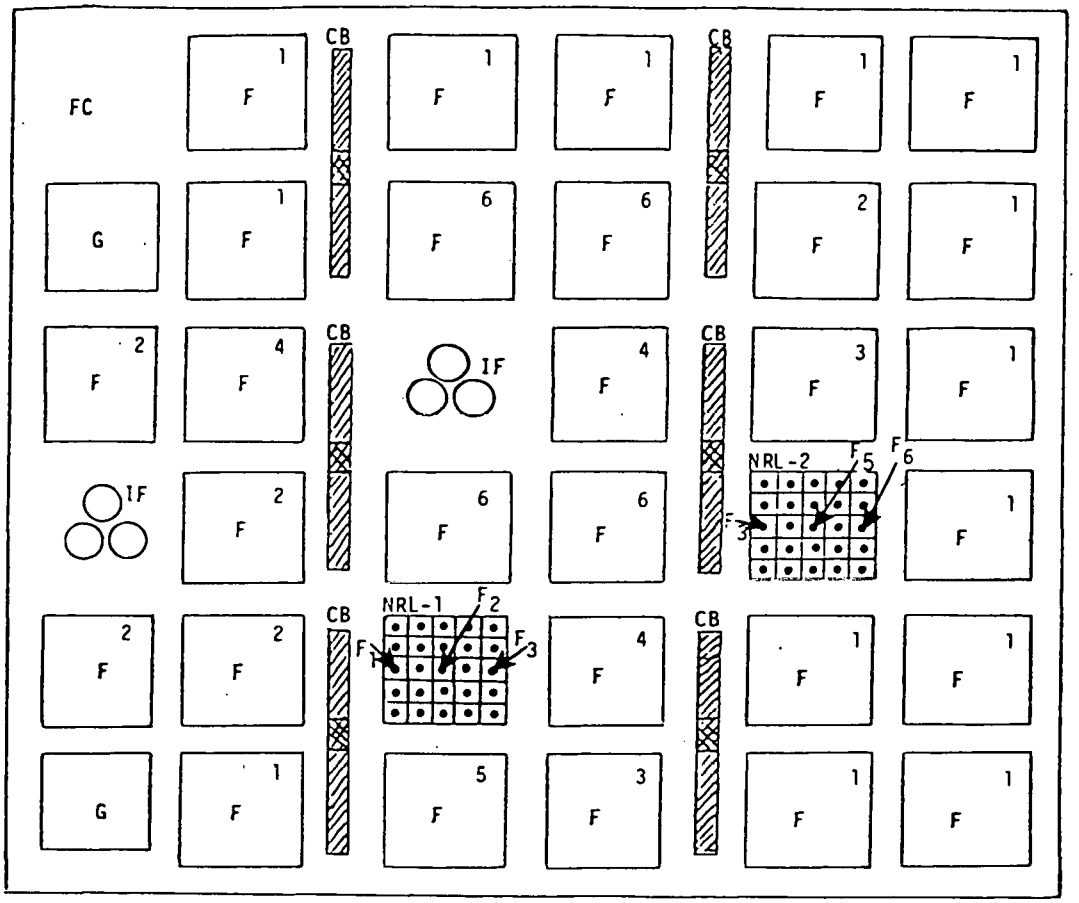

Control Rod Blade Channel (Fuel Row)

Control Rod Blade Channel (Water Row)

G Graphite

FC Fission Chamber

F Fuel Subassembly

F_1, F_2, F_3, F_4, F_5 and F_6 Representative Test Positions

IF Isotope Facility

NRL Naval Research Laboratory Irradiation Facility (approximately 8Kg of steel in each)

Number in right-hand corner of subassembly is composition number.

FIGURE 1. Nuclear Test Reactor Model.

Fuel Compositions

The atom densities of the six different types of fuel compositions were calculated using a cell model consisting of a cladded fuel pin surrounded by water. The arrangement of fuel and water was enclosed by a ring of heavy scatterer material.

The area of the water in the cell was made equivalent to 1/25 of the cross sectional area of the water in the subassembly. Similarly, the area of the cladding surrounding the fuel pin was taken as the sum of the areas of the fuel cladding and 1/25 the cross sectional area of the subassembly shell.

The fuel pin was characterized, on the basis of the normal operating power of 2 MW and a fuel loading of 564.7 gm UO_2 per pin. However, to establish the fuel composition, it was necessary to deplete the fresh fuel composition in the fuel pin of the cell using depletion time steps of various lengths. The length of a depletion time step was established from:

$$\text{Power density} = 4.16 \times 10^{-5} \text{ MW/cm}$$
$$\text{Linear density} = 8.51 \times 10^{-6} \text{ Tons/cm.}$$

For example, the number of days of exposure required to achieve a burnup of 10,474 MWd/T was calculated as:

$$2{,}143 \text{ days} = 10{,}474 \frac{\text{MWd}}{\text{T}} \times \frac{8.51 \times 10^{-6} \text{ T}}{4.16 \times 10^{-5} \text{ MW}}.$$

Starting with the fresh fuel composition identified as Composition 0, fuel compositions corresponding to six burnup values ranging from 436 to 10,474 MWd/T were computed. The homogenized fuel compositions required in the core model, Figure 1, were obtained from these results.

The parameters used with each fuel composition were 28-group resonance and spatially self-shielded cross sections. Six different sets of 28-group cross sections were generated as follows.

Homogeneously resonance self-shielded cross sections for each fuel composition were derived from a unit cell calculation using the one-dimensional diffusion theory code, 1DX [5]. The geometry of the cell was a cylinder with reflecting boundary conditions shown by the radial configuration of Figure 2. The resonance self-shielded cross sections were computed for the homogenized fuel composition of zone Z_4 of Figure 2.

The cross sections used in the 1DX [5] calculation consisted of a 30 energy group set derived from Set 300 [2]. However, the integral-scattering terms for hydrogen were modified to provide a correct treatment of the slowing down of neutrons by water during the calculation. The resonance self-shielded cross sections derived from this calculation were collapsed to a 28-group set for further processing.

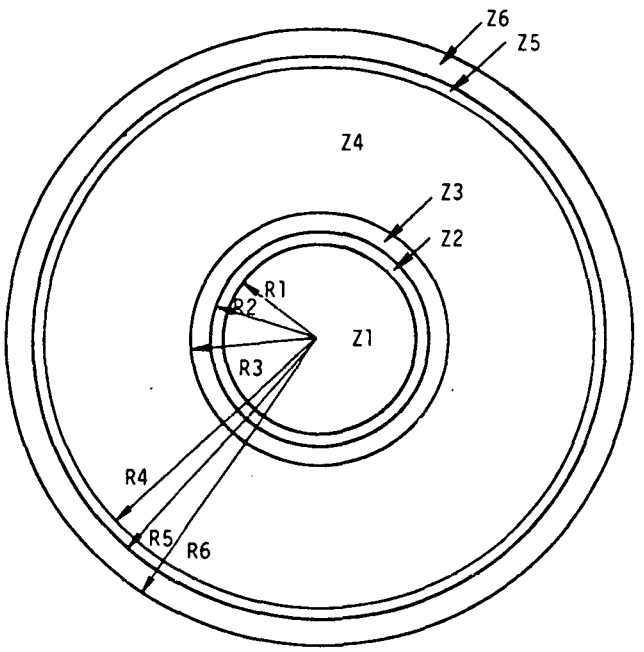

R_1 = 0.5518 cm
R_2 = 0.60198 cm
R_3 = 0.75006 cm

Z_1 = Fuel Pin
Z_2 = Clad
Z_3 = Interstitial Water

R_4 = 3.750245 cm
R_5 = 4.210075 cm
R_6 = 4.29985 cm

Z_4 = Homogenized Fuel (water, clad, fuel from all pins other than center pin)
Z_5 = Zircaloy Box
Z_6 = Water Separating Subassemblies

FIGURE 2. Fuel Cell Model.

Resonance self-shielded cross sections were utilized in the transport theory code DTF-IV [3] to generate a set of spatially self-shielded cross sections for each fuel material composition. The calculations were performed using the model shown in Figure 2.

Using DTF-IV in cylindrical geometry with reflecting boundary conditions, fine-structured multigroup fluxes were calculated through the cell of Figure 2. The space-energy fluxes calculated in this manner were used to form flux- and volume-weighted effective multigroup cross sections for each material in the fuel pin. These cross sections were then used in a second DTF-IV calculation in which the fuel pin compositions were smeared in with those of the homogeneous fuel regions of Figure 2. This latter calculation provided a set of effective multigroup cross sections appropriate for the subassembly compositions of Figure 1.

RESULTS

Flux Calculations

The space-energy fluxes in the irradiation zones of Figure 1 (marked NRL zones) were computed using the atom densities for Compositions 1 through 6 in the two-dimensional diffusion theory code 2DBS [1]. Each fuel zone (F zone) in Figure 1 is identified by the composition number in the right-hand corner of the homogenized fuel zone.

The fluxes in each NRL zone were calculated at 25 mesh points indicated in the NRL-1 and NRL-2 zones of Figure 1. Typical flux variations throughout the zones are characterized by the flux shapes given in Figure 3 for test positions F_1, F_2, and F_3, and in Figure 4 for test positions F_4, F_5, and F_6.

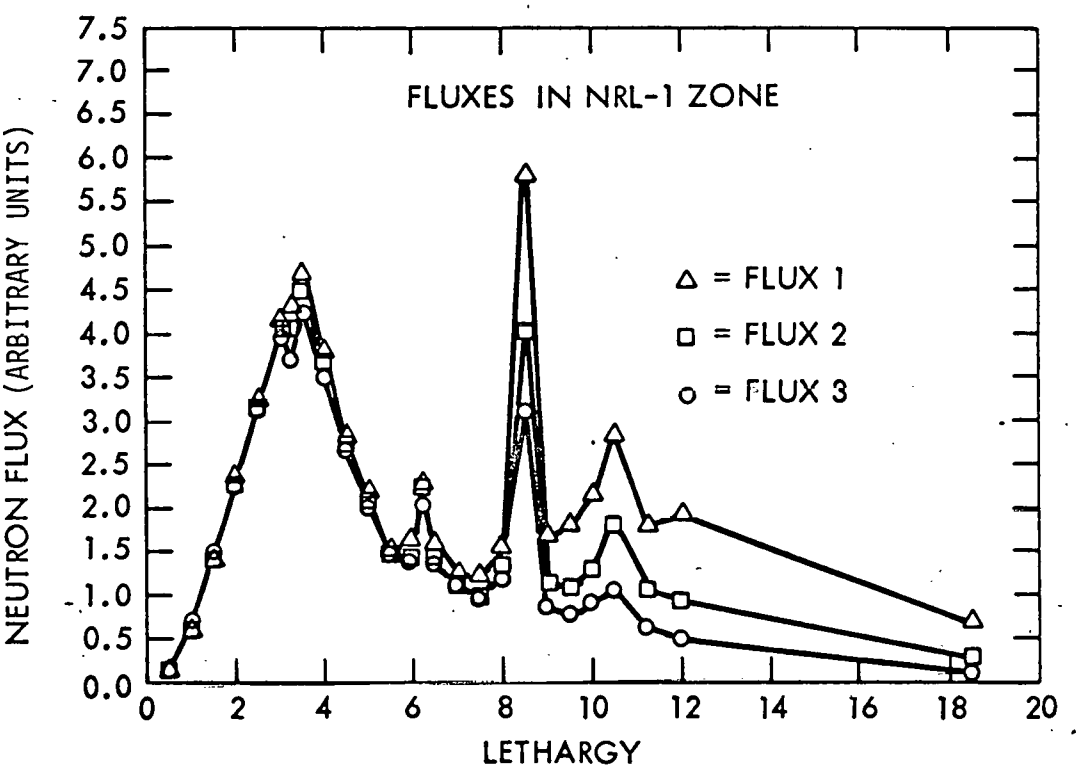

FIGURE 3. Flux Variations Through NRL-1 Test Assembly.

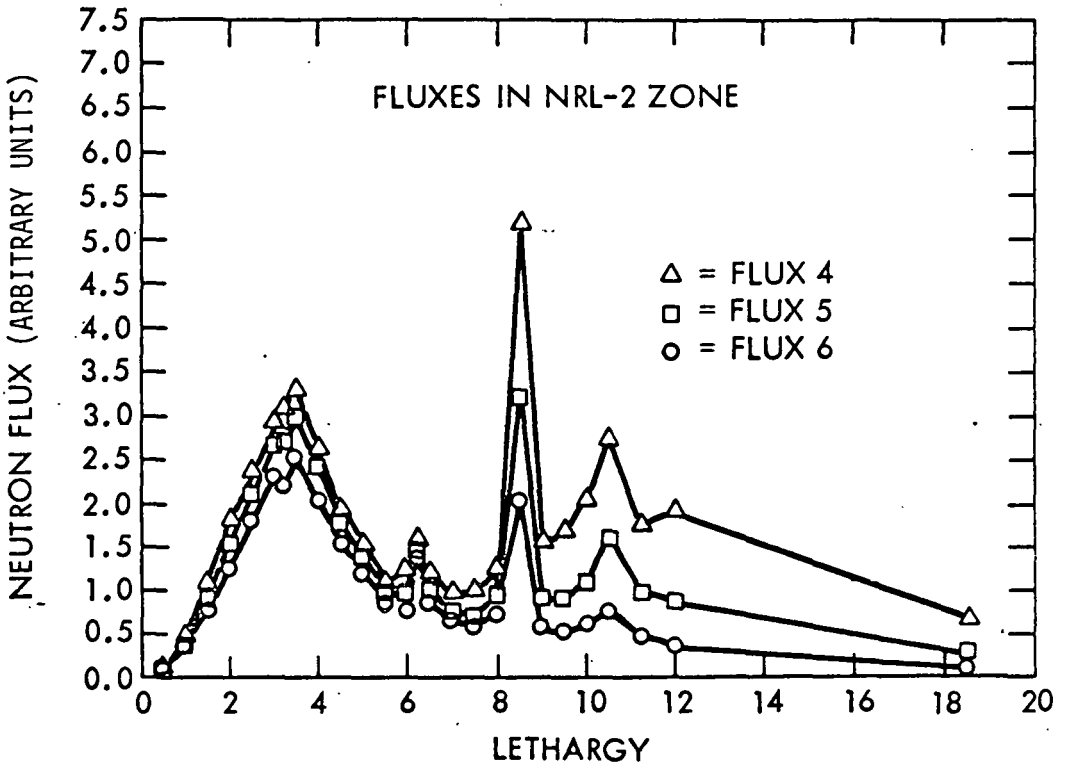

FIGURE 4. Flux Variations Through NRL-2 Test Assembly.

The 28-group fluxes at the designated positions of each test zone were expanded to a 620-point spectrum using the SAND-II code [6]. The expanded spectrum was then used to calculate spectrum-averaged cross sections as follows.

$$\bar{\sigma} = \int_0^{18\ \text{MeV}} \sigma(E)\phi(E)dE \Big/ \int_0^{18\ \text{MeV}} \phi(E)dE = \int_0^{18\ \text{MeV}} \sigma(E)\phi(E)dE \Big/ \phi_{\text{Total}}$$

where, $\bar{\sigma}$ is the spectrum-averaged reaction cross section, $\sigma(E)$ is the energy-dependent reaction cross section, and $\phi(E)$ is the flux spectrum distribution. In addition, the spectrum-averaged cross sections referred to the fluxes with energies greater than 0.1 MeV, 0.5 MeV, and 1.0 MeV, are given by:

$$\frac{\int_{0}^{18\ \text{MeV}} \sigma(E)\phi(E)dE}{\int_{E>X}^{18\ \text{MeV}} \phi(E)dE} = \frac{\overline{\sigma\phi}_{\text{Total}}}{\phi_{E>X}} \qquad (2)$$

where X is cut-off values 0.1, 0.5, and 1.0 MeV.

Using the 620-point fluxes evaluated at the test positions F_1 through F_6, and Equation (2), integrated fluxes, spectrum-averaged cross sections for the $^{54}Fe(n,p)^{54}Mn$ and $^{58}Ni(n,p)^{58}Co$ reactions and the displacement cross sections for iron and stainless steel were calculated for energy ranges greater than 0.1, 0.5, and 1.0 MeV. These results are presented in Table I.

For comparison purposes, additional flux calculations were performed on a uniform burnup model of the test reactor in which a burnup of 7,000 MWd/T was assumed in all regions of Figure 1.

CONCLUSIONS

The fluxes obtained from the nonuniform burnup model, shown in Table I, are larger at the left edge than at the center and right edge of each test subassembly. In addition, they are lower in magnitude than the fluxes obtained with the uniform burnup model. In this model, the fluxes are peaked at the center of each test subassembly.

The general effect of the nonuniform burnup model is to predict lower fluxes and average cross sections at the center of each test subassembly than those predicted by the uniform burnup models. The conclusions derived from these analyses are:

1. The calculations must be modeled to correctly include burnup, otherwise one can obtain order of magnitude differences in calculated fluxes greater than 1 MeV, normally used for correlation of measured property changes.

2. Fluence values based on measured reaction rates and calculated values of spectral-averaged cross sections greater than 1 MeV will be as much as 10 to 15 percent too high if burnup effects are neglected.

TABLE I

BUFFALO LWR CALCULATION RESULTS

Parameter	Integration Range	F-1 NRL-1 Position 4-B	F-2 NRL-1 Position 4-B	F-3 NRL-1 Position 4-B	F-4 NRL-2 Position 2-C	F-5 NRL-2 Position 2-C	F-6 NRL-2 Position 2-C
ϕ*	Total	31.4	24.1	20.1	26.1	17.7	12.4
	E>0.1 MeV	11.8	11.3	11.2	8.43	7.50	6.35
	E>0.5 MeV	5.92	5.74	5.84	4.36	3.82	3.24
	E>1.0 MeV	3.21	3.11	3.28	2.44	2.09	1.75
$(\bar{\sigma})$Fe54	Total	7.02×10^{-27} cm^2	8.89×10^{-27} cm^2	1.25×10^{-26} cm^2	6.63×10^{-27} cm^2	8.12×10^{-27} cm^2	1.00×10^{-26} cm^2
	E>0.1 MeV	1.87×10^{-26} "	1.87×10^{-26} "	2.25×10^{-26} "	2.06×10^{-26} "	1.91×10^{-26} "	1.96×10^{-26} "
	E>0.5 MeV	3.72×10^{-26} "	3.73×10^{-26} "	4.28×10^{-26} "	3.97×10^{-26} "	3.75×10^{-26} "	3.84×10^{-26} "
	E>1.0 MeV	6.87×10^{-26} "	6.90×10^{-26} "	7.65×10^{-26} "	7.09×10^{-26} "	6.87×10^{-26} "	7.10×10^{-26} "
$(\bar{\sigma})$Ni58	Total	9.71×10^{-27} cm^2	1.23×10^{-26} cm^2	1.71×10^{-26} cm^2	9.17×10^{-27} cm^2	1.12×10^{-26} cm^2	1.39×10^{-26} cm^2
	E>0.1 MeV	2.59×10^{-26} "	2.61×10^{-26} "	3.08×10^{-26} "	2.84×10^{-26} "	2.65×10^{-26} "	2.69×10^{-26} "
	E>0.5 MeV	5.14×10^{-26} "	5.15×10^{-26} "	5.86×10^{-26} "	5.48×10^{-26} "	5.19×10^{-26} "	5.28×10^{-26} "
	E>1.0 MeV	9.50×10^{-26} "	9.53×10^{-26} "	1.045×10^{-25} "	9.79×10^{-26} "	9.50×10^{-26} "	9.77×10^{-26} "
$(\bar{\sigma})$Nat.Fe Disp.	Total	1.84×10^{-22} cm^2	2.30×10^{-22} cm^2	2.81×10^{-22} cm^2	1.64×10^{-22} cm^2	2.09×10^{-22} cm^2	2.50×10^{-22} cm^2
	E>0.1 MeV	4.90×10^{-22} "	4.87×10^{-22} "	5.07×10^{-22} "	5.07×10^{-22} "	4.92×10^{-22} "	4.88×10^{-22} "
	E>0.5 MeV	9.73×10^{-22} "	9.62×10^{-22} "	9.64×10^{-22} "	9.81×10^{-22} "	9.64×10^{-22} "	9.58×10^{-22} "
	E>1.0 MeV	1.76×10^{-21} "	1.78×10^{-21} "	1.72×10^{-21} "	1.75×10^{-21} "	1.77×10^{-21} "	1.77×10^{-21} "
$(\bar{\sigma})$SS Disp.	Total	1.92×10^{-22} cm^2	2.40×10^{-22} cm^2	2.93×10^{-22} cm^2	1.71×10^{-22} cm^2	2.13×10^{-22} cm^2	2.62×10^{-22} cm^2
	E>0.1 MeV	5.13×10^{-22} "	5.09×10^{-22} "	5.29×10^{-22} "	5.30×10^{-22} "	5.14×10^{-22} "	5.10×10^{-22} "
	E>0.5 MeV	1.02×10^{-21} "	1.01×10^{-21} "	1.01×10^{-21} "	1.03×10^{-21} "	1.01×10^{-21} "	1.00×10^{-21} "
	E>1.0 MeV	1.88×10^{-21} "	1.86×10^{-21} "	1.80×10^{-21} "	1.83×10^{-21} "	1.85×10^{-21} "	1.85×10^{-21} "

*Relative neutron fluxes arbitrary units.

Correlation of the calculated flux with measurements or other calculations will enable accurate fluence determinations for the NRL irradiation. The detailed fluence spectra will be used in damage analysis to correlate damage data from the Buffalo reactor with those obtained in other LWR or fast reactor test irradiations.

REFERENCES

[1] MARR, D.R., A User's Manual for 2DBS, A Diffusion Theory Shielding Code, BNWL-1291, Pacific Northwest Laboratories, Richland, WA (February 1970).

[2] SCHENTER, R.E., KIDMAN, R.B., and NELSON, J.V., FTR Set 300, Multigroup Cross Sections for FTR Design, HEDL-TME 71-153, Hanford Engineering Development Laboratory, Richland, WA (October 1971).

[3] LATHROP, K.D., DTF-IV, A Fortran-IV Program for Solving the Multigroup Transport Equation With Anisotropic Scattering, A-3373, Los Alamos Scientific Laboratory, Los Alamos, NM (1965).

[4] PONCELET, C.G., LASER - A Depletion Program for Lattice Calculations Based on MUFT and THERMOS, WCAP-6073, Westinghouse Electric Power Division, Atomic Power Division, Pittsburgh, PA (April 1966).

[5] HARDIE, R.W. and LITTLE, JR., W. W., 1DX, A One-Dimensional Diffusion Theory Code for Generating Effective Nuclear Cross Sections, BNWL-954, Pacific Northwest Laboratories, Richland, WA (September 1968).

[6] McELROY, W.N. and BERG, S., A Computer-Automated Iterative Method for Neutron Flux Spectra Determined by Foil Activations, Vol. I-IV, AFWL-TR-67-41, Air Force Weapons Laboratory, Kirkland AFB, NW (1967).